

# From *In Situ* Monitoring to Better Understanding of the Suzuki-Miyaura Cross Coupling in the Solid State

Mario Pajić,<sup>[a]</sup> Dajana Barišić,<sup>[a, b]</sup> Darko Babić,<sup>[a]</sup> Manda Ćurić,<sup>[a]</sup> and Marina Juribašić Kulcsár\*<sup>[a]</sup>

Effects of various Additives, Base, Catalyst, as well as substrates on the mechanochemically-induced Suzuki-Miyaura reaction have been studied. *In situ* Raman monitoring of the solid-state reactions gave a detailed view of the reaction course and allowed a direct comparison of the time-resolved product

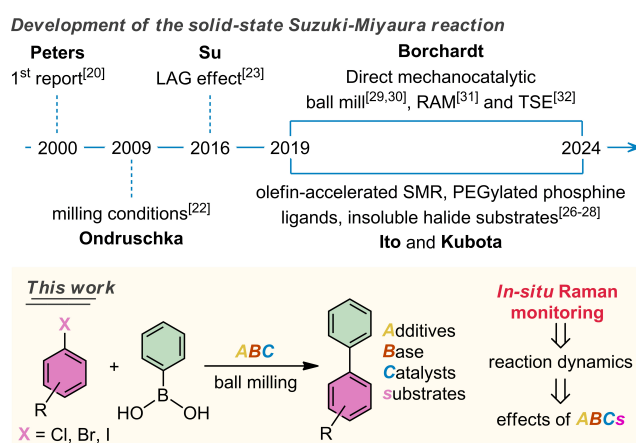
formation. The acquired knowledge allows in-depth understanding of the reaction, especially the action of the catalyst in presence of diverse chemicals, leading to the more efficient cross coupling reactions in the solid state.

## Introduction

The palladium-catalyzed coupling of alkenyl boranes with organic bromides, first published in 1979,<sup>[1]</sup> developed into one of the key reactions for the construction of carbon-carbon (C–C) bonds in modern organic chemistry – the Suzuki-Miyaura reaction (SMR). The pioneering work<sup>[1]</sup> laid ground for many other studies that improved the method for the coupling of boron compounds and organic halides.<sup>[2,3]</sup> The immense importance of this discovery led to Akira Suzuki being awarded the Nobel Prize in Chemistry in 2010. The interest in improving this versatile coupling method keeps growing due to its wide application in the chemical industry, drug discovery, and material science. The reaction scope has been expanded to various substrates and less reactive coupling partners, while the catalyst loadings have been reduced.<sup>[2,3]</sup> In many cases, these advances rely on increasing the catalyst's reactivity and stability by adding tailored phosphine-based ligands, which are toxic, expensive, and often only available by synthesis.<sup>[2,5]</sup> To make SMR more environmentally friendly and acceptable for the pharmaceutical processes, other catalytic systems like *N*-heterocyclic carbene (NHC) palladium complexes,<sup>[3,6–8]</sup> palladacycles<sup>[3,6,9,10]</sup> or palladium nanoparticles (PdNPs),<sup>[3,6,9–13]</sup> as well as the “ligandless” approach<sup>[12]</sup> or the aqueous reaction media<sup>[6,14]</sup> have been explored. The ultimate goal is to reduce the catalyst loading, recycle the metal used, and avoid harmful additives, including solvents, to make the coupling meet the standards of green chemistry principles.<sup>[15,16]</sup>

In this context, solid-state synthetic methods, in particular ball milling,<sup>[17–19]</sup> that enable chemical transformations without a solvent medium, are gaining attention. Higher yields and better selectivity can be achieved in a shorter reaction time, making these reactions eco-friendlier.<sup>[17–19]</sup> Moreover, the solid-state approach circumvents the challenges associated with solubility, concentration-dependent phenomena, and solute-solvent effects that can affect the reaction course in solution-based chemistry.<sup>[17–19]</sup> The reduced use of solvents typically lowers the overall cost and increases the green chemistry metrics of the reaction.<sup>[15,16]</sup>

Since their initial reports in the 2000s,<sup>[20–23]</sup> the solid-state methods have proved remarkably versatile and have been expanded to Suzuki-Miyaura cross coupling of the most demanding substrates, regardless of their aggregate state or solubility (Scheme 1),<sup>[24,25]</sup> This adaptability has been further demonstrated in the last five years by ball milling, which has made this methodology readily available for diverse uses.<sup>[26–31]</sup> Insoluble and complex substrates which do not react in solution can be rapidly converted to products in high yields by ball milling.<sup>[26]</sup> Moreover, there is no need for inert conditions<sup>[20–31]</sup> and, in some cases, for the addition of the catalyst as the reaction can occur on the surface of the palladium milling



**Scheme 1.** Solid-state Suzuki-Miyaura reaction studies till date and in this work.

[a] Division of Physical Chemistry, Ruđer Bošković Institute, Zagreb, Croatia  
[b] Selvita Ltd. Zagreb, Zagreb, Croatia

**Correspondence:** Dr. Marina Juribašić Kulcsár, Division of Physical Chemistry, Ruđer Bošković Institute, Bijenička cesta 54, Zagreb HR-10000, Croatia.  
Email: marina.juribasic@irb.hr

Supporting Information for this article is available on the WWW under <https://doi.org/10.1002/cmt.202400025>

© 2024 The Author(s). Chemistry - Methods published by Chemistry Europe and Wiley-VCH GmbH. This is an open access article under the terms of the Creative Commons Attribution License, which permits use, distribution and reproduction in any medium, provided the original work is properly cited.

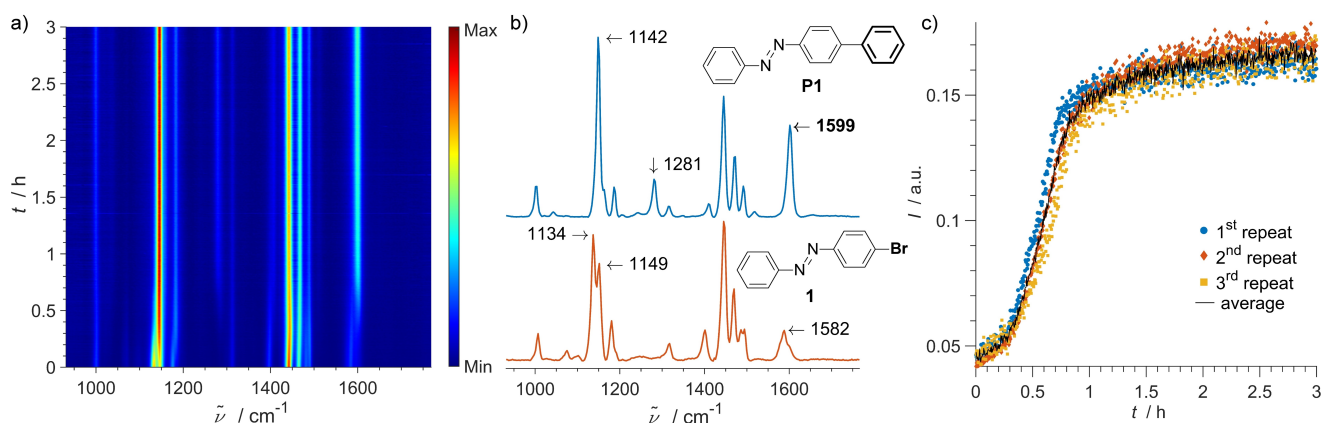


**Figure 1.** a) 2D plot of the time-resolved Raman monitoring of the mechanochemically-induced Suzuki-Miyaura coupling of **1** (0.40 mmol) with PBA (0.52 mmol) catalyzed by **C1** (0.050 equiv.) using  $K_2CO_3$  (0.96 mmol) as the base and silica (250 mg) as the milling auxiliary ("standard conditions"). b) Selected part of the Raman spectra of **1** and **P1** with their characteristic bands. c) Time-resolved Raman intensities at  $1599\text{ cm}^{-1}$  for the replicated reactions and a line plot of their average.

balls.<sup>[29,30]</sup> More recently, other solid-state methods, such as resonant acoustic milling (RAM),<sup>[31]</sup> twin-screw extrusion (TSE),<sup>[32–34]</sup> and electromagnetic ball milling,<sup>[35]</sup> have also shown promise in the Suzuki-Miyaura cross coupling. Despite these advancements, the mechanistic insight into the solid-state process still relies on the *ex situ* data.<sup>[20–31]</sup>

Functionalization of organic substrates usually requires addition of various compounds into the reaction mixture. As the reaction mixture gets more complex, various potentially obstructive interactions or side reactions between components might occur. In this context, comparable data on the impact of additives on the reaction course is needed for a rational reaction design. Although it is one of the oldest known mechanochemically-induced reactions forming a new covalent bond, factors affecting the course and the product formation dynamics of the Suzuki-Miyaura cross coupling have never been investigated *in situ*.

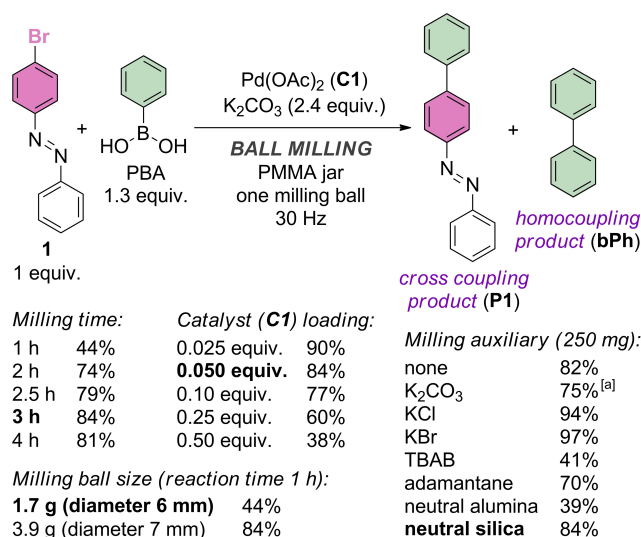
To address this limitation, the mechanochemically-induced Suzuki-Miyaura reaction was monitored *in situ* by the solid-state Raman spectroscopy<sup>[36,37]</sup> allowing for the first time a direct insight to the effects that the reaction participants have on the product formation. Effects that essential ABCs, *i.e.*, Additives, Bases, Catalysts and substrates, have on the reaction course and outcome in the solid state have been analyzed (Scheme 1). Future design of the solid-state coupling reactions will benefit from the acquired deeper understanding of the key factors affecting the reaction.

## Results and Discussion

Mechanochemically-induced reactions can be monitored *in situ* and in real time by the solid-state Raman spectroscopy (Figure 1a).<sup>[36,37]</sup> *In situ* monitoring is a prerequisite for reliable insight into the reaction dynamics without stopping the milling process and opening the milling jar, which may change the course of the solid-state reaction.<sup>[36,37]</sup> High-quality Raman data are obtained with a substrate and/or a product that exhibit

strong Raman bands to reduce the influence of additional compounds introduced into the reaction mixture (additives) onto the spectrum of the reaction mixture. Thus, we first searched for the appropriate SMR substrate to meet these requirements.

Based on our experience in the solid-state Raman monitoring,<sup>[38–45]</sup> 4-bromoazobenzene (**1**) with a highly Raman-active phenyl and azo (N=N) groups was selected as a model substrate (Scheme 2). After coupling with phenylboronic acid (PBA), **1** is converted to 4-phenylazobenzene (**P1**). Solid-state Raman spectra of **1** and **P1** (Figure 1b) contain several bands around  $1450\text{ cm}^{-1}$ , which have a strong contribution of the azo bond (N=N) stretching. These bands are not significantly altered during the reaction. In contrast, two bands of the phenyl ring vibrations of **1** at  $1134$  and  $1149\text{ cm}^{-1}$  merge into a strong band



**Scheme 2.** Screening of milling conditions (auxiliary, time, and ball size) for the Suzuki-Miyaura reaction of **1** and PBA assessed by NMR yields for **P1**. One parameter was changed in each trial with regard to standard conditions (marked in bold), except for the milling ball size. <sup>[a]</sup> 1.0 gram of  $K_2CO_3$  was used.

at  $1142\text{ cm}^{-1}$  for **P1**. A medium-intensity band at  $1281\text{ cm}^{-1}$ , assigned to the stretching of the C–C bond between two phenyl rings, is characteristic for **P1**. The most prominent difference in the spectra of the substrate and the coupling product is in the phenyl C=C stretching band, present at  $1582\text{ cm}^{-1}$  for **1** and at  $1599\text{ cm}^{-1}$  for **P1**.

Other compounds in the mixture, *i.e.*, the catalyst, PBA, the base, additives, side products (biphenyl (**bPh**), and benzene), and various byproducts are present in a small amount and/or exhibit low-intensity Raman spectra and therefore do not contribute significantly to the collected spectra. Moreover, activation of the C–H bonds in the available organic compounds by palladium is possible under examined experimental conditions,<sup>[40–42]</sup> but it was not detected by *in situ* or *ex situ* methods.

Another relevant feature in solution-based and solid-state synthesis is the effect of additives that can affect the reaction course. Additives often tune the solid-state reaction and improve its outcome.<sup>[17–19]</sup> Using a liquid additive instead or along with the solid additive (*e.g.*, salts or polymers) may have a profound effect on the solid-state reaction that is not observed in the solution.<sup>[17–19]</sup> Methods known as liquid-assisted grinding (LAG), ion-assisted grinding (IAG), ion-and-liquid-assisted grinding (ILAG), and polymer-and-liquid-assisted grinding (POLAG) can be faster and achieve better yields than the analogous reactions without additives (*i.e.* neat grinding, NG).<sup>[17–19]</sup>

We started with a common Pd-catalyst palladium(II) acetate (**C1**, Pd(OAc)<sub>2</sub>, 0.050 equiv. with regard to **1**) and potassium carbonate (K<sub>2</sub>CO<sub>3</sub>, 2.4 equiv.) as a base, to achieve coupling of **1** (1 equiv.) with PBA (1.3 equiv.) (Scheme 2). A high yield (82%) was obtained in 3 hours, but the quality of the Raman data was low due to the partial formation of a compact reaction mixture that was not mixing properly.

In mechanochemical ball milling reactions, it is important not to overload the reaction mixture with a liquid to avoid slurries. In this context, adding an inert solid as a milling auxiliary can help keep the reaction mixture dry and homogeneous. Thus, we screened the milling auxiliaries to obtain a favorable rheology of the reaction mixture that would not stick to the walls of the milling jar and/or the milling ball. Such reaction mixture would provide reproducible reaction conditions and good-quality Raman monitoring.

Various substances were tested as milling auxiliaries, including inorganic salts (KCl, KBr, K<sub>2</sub>CO<sub>3</sub>), an organic inert solid (adamantane), tetrabutylammonium bromide (TBAB, a surfactant known for its stabilization of PdNPs<sup>[13]</sup>), neutral alumina (Al<sub>2</sub>O<sub>3</sub>) and neutral silica (SiO<sub>2</sub> (Scheme 2). Among these, the reaction mixture with silica stood out. It was not only homogeneous and easy to handle (Figure S5) but also provided a nicely resolved Raman data throughout milling (Figure 1a). This led us to select silica as a milling auxiliary for further experiments.

Milling time and catalyst loading were screened next to obtain a well-resolved Raman monitoring of the reaction that allows yield improvement (Scheme 2, Tables S1–S5). According to the collected data, milling of a mixture of **1** (1 equiv.) and

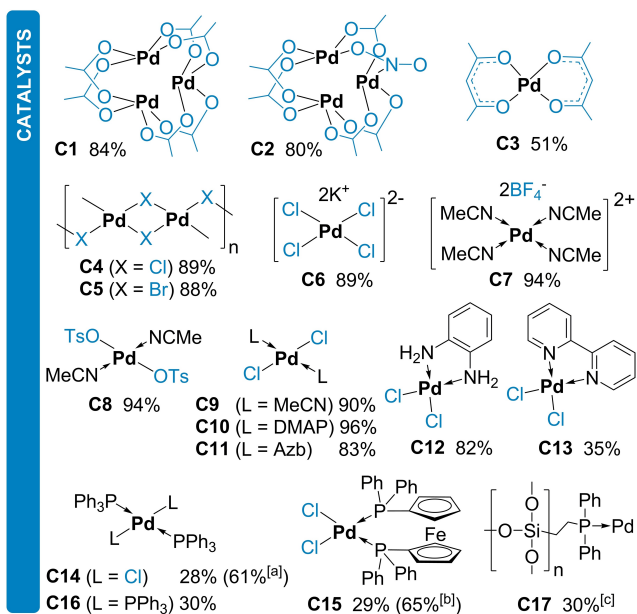
PBA (1.3 equiv.) with the catalyst (0.050 equiv.) and K<sub>2</sub>CO<sub>3</sub> (2.4 equiv.) along with the silica auxiliary (250 mg) for 3 hours using one nickel-bound tungsten carbide (WC) milling ball (diameter 6 mm, 1.7 g) was selected as “standard conditions” for further experiments.

The product formation in the studied SMR was followed by *in situ* Raman monitoring<sup>[36,37]</sup> (Figure 1c). A reaction profile showing the time-dependent evolution of the Raman band at  $1599\text{ cm}^{-1}$ , characteristic of the product **P1**, was used to follow the reaction course (Figure 1c). The time-resolved product formation displayed distinct differences with various additives, bases and catalysts. This allowed the study of the impact the structure of the catalyst, as well as acid-base properties, and the aggregate state of the additives and the base, have on the reaction efficiency. The reproducibility of the reaction profiles was checked by occasional repeating of the selected reactions. In most profiles no significant amount of the product was formed at the beginning of milling. This induction period varied in duration (from 5 to 50 minutes), and suggested that some preparation for the coupling was occurring *in situ*. These results could be attributed to (i) the activation of PBA by the formation of borate species needed in the transmetalation or (ii) the transformation of the employed complex (pre-catalyst) into the active catalytic species. Apart from the ligand change and reduction of the employed Pd(II) complex to form an active Pd(0) catalyst (if needed), formation of the hydroxo Pd-species is usually necessary for the successful transmetalation.<sup>[5,46–51]</sup>

To gain a better insight, a two-step reaction was performed. Compounds **1**, PBA, and K<sub>2</sub>CO<sub>3</sub> were milled for 1 hour. Then, the catalyst **C1** was added, and milling was continued for 3 hours. The Raman profile of this second step showed a similar initiation period, although the activation of PBA probably already occurred in the first step (Figure S29). This indicates that the change in the catalyst is the likely cause of the initial slow product formation. In addition, this experiment suggests that no deterioration of the reaction components occurs when they are milled without the catalyst.

*In situ* Raman and *ex situ* <sup>1</sup>H NMR spectra of the reaction mixtures recorded during the initiation period show no azobenzene *N*-coordinated to the palladium, although **1** is in significant excess. Therefore, the initiation period cannot be attributed to the coordination of the available azobenzenes to the palladium. Another possibility for the delay in product formation is activation of the catalyst, either as a loss or exchange of the ligands. The elimination of the ligand depends on the bond strength of the ligand. MeCN is loosely bound to palladium, consistent with the *in situ* observed initiation period of less than 10 minutes for MeCN complexes **C7–C9** (Scheme 3). In contrast, initiation for **C10–C16** takes more than 40 minutes. Thus, labile ligands that are initially bound to the metal make the activation of the pre-catalyst easier.

To gain more insight, we employed SiliaCat DPP-Pd (**C17**), a highly reactive and reusable silica-based heterogeneous diphenylphosphine palladium(II) catalyst for the cross coupling reactions in solution.<sup>[52]</sup> According to the Raman monitoring of the solid-state SMR using our experimental setup and SiliaCat DPP-Pd (Figure 2d), the observed time-resolved product for-



**Scheme 3.** Catalysts C1–C17 and NMR yields for SMR under standard conditions catalyzed by C1–C17. <sup>[a]</sup> Reaction time was 12 hours. <sup>[b]</sup> LAG using 2.4 equiv. of water. <sup>[c]</sup> Average of two runs. Anions are marked blue.

mation is comparable to those observed in the reactions catalyzed by PdCl<sub>2</sub>(bpy) (C13) and the phosphine catalysts. If no substrate is available, the activated Pd-species may deteriorate in agreement with the results of the two-step reaction, in which, PBA was added to the mixture in the second step.

**Side reactions.** Three reactions can occur in the examined system. The desired Suzuki-Miyaura cross coupling could be accompanied by two side reactions involving boronic acids: oxidative homocoupling and protodeboronation. In most cases, the *ex situ* <sup>1</sup>H NMR spectra of the crude reaction mixtures showed the unreacted substrate **1**, the product **P1**, usually a small amount of biphenyl (**bPh**) and, in some cases, benzene, a protodeboronation product. The detection of **bPh** as the primary side product indicated that homocoupling of PBA was the dominant side reaction. If we compared the amounts of **P1** and **bPh** with the amount of PBA introduced to the reaction mixture, in most reactions no significant amount of PBA was protodeboronated corroborated by the observed small amount of the benzene (**PhH**) in the reaction mixtures (usually less than

2% of PBA was transformed to **PhH**, Tables S1–S4). This was more pronounced only in reactions using adamantane and Al<sub>2</sub>O<sub>3</sub> as the milling auxiliary (4% yield for **PhH**), and in the reaction catalyzed by the silica-based catalyst **C17** (3% yield for **PhH**).

*Oxidative homocoupling* could not be avoided in our experimental setup. The reaction catalyzed by **C1** with 1.0 equiv. of PBA in regard to **1** ends with a lower yield of **P1** (77%) but still affords **bPh** (Table S1). Moreover, the amount of **bPh** in the reaction mixture is higher if the loading of **C1** is increased above 0.050 equiv. to **1** (as under standard conditions). This leads to **bPh** being the major product in the reaction with the **C1** loading of 0.25 equiv. to **1** and higher.

The homocoupling usually proceeds *via* the peroxy-palladium species formed by bonding of the oxygen (O<sub>2</sub>) to the palladium catalyst.<sup>[53]</sup> According to the *ex situ* <sup>1</sup>H NMR monitoring of the SMR of **1** catalyzed by **C1** under standard conditions (Figure S51), the homocoupling product **bPh** is present almost from the start of milling. Sampling of the reaction mixture for the NMR monitoring was performed by opening of the jar and thus introducing oxygen (from the air) each time to the reaction system. However, no significant amount of **bPh** was formed after the initial period. A change in the selectivity in the course of the reaction should occur either due to a change of the active catalyst (homocoupling to SMR catalyst) or due to a change of the catalyst amount (if the side homocoupling proceeds as the second-order reaction and the cross coupling as the first-order one). Taking into account that a significant amount of PBA (along with **1**) was left unreacted in some trials with a poor outcome for both **P1** and **bPh**, we hypothesize that the conversion of the active catalyst for the homocoupling to the active SMR catalyst is more in line with the experimental data.

Milling of PBA, **C1**, and K<sub>2</sub>CO<sub>3</sub> with silica (no SMR substrate) for 3 hours as well as the reaction under standard conditions using the chlorosubstrates (4-chloroazobenzene (**2**) and 4-chloroaniline (**7**), *vide infra*) results in the exclusive formation of **bPh**. These results indicate that the palladium species catalyzing the homocoupling forms and is active in the absence of the valid SMR substrate.

To check the catalyst deterioration, we have performed the reaction without PBA. Substrate **1** (1 equiv.), **C1**, K<sub>2</sub>CO<sub>3</sub>, and silica were milled for one hour. Then PBA (1.3 equiv.) was added, and the obtained mixture was milled for 3 hours more.

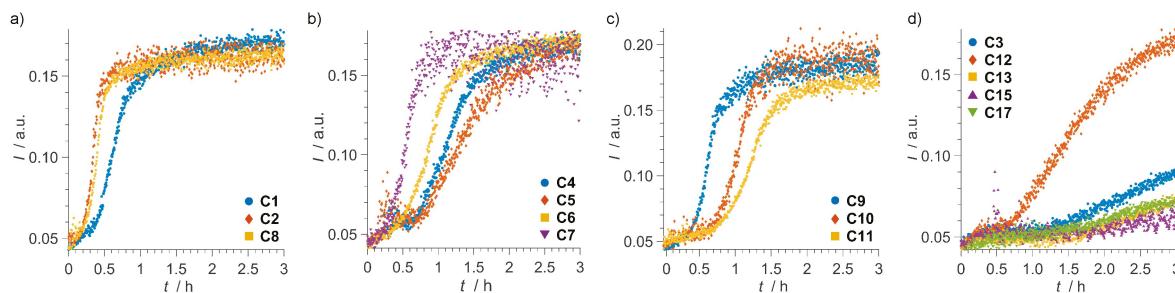


**Figure 2.** Time-resolved Raman intensities at 1599 cm<sup>-1</sup> for the coupling using a) O-ligand catalysts (C1, C2 and C8), b) halide catalysts (C4–C7), c) dichloride catalysts (C9–C11), and d) catalysts with the chelating ligands (C3, C12, C13 and C15) and the silica-based catalyst C17.



The yield for **P1** in this reaction sequence is only 24% showing that most of the catalyst was deactivated in the first step where no boronic acid was present. A possible reaction during the first step, except ligand bonding<sup>[40–42]</sup> or anion metathesis<sup>[43]</sup> in the catalyst, is the oxidative addition of the SMR substrate to the palladium species. As no boronic coupling partner was present, this species might have changed irreversibly forming less active or even inactive palladium catalyst for both, the homo- and the cross coupling.

To check the activity of the catalyst after 3 hours of milling under standard conditions, we have performed the two-step one-pot reaction. The first step was conducted under standard conditions producing **P1** (and **bPh**) as in Figure 1c. Then, 1 equiv. of **1** along with PBA (1.3 equiv.) and  $K_2CO_3$  (2.4 equiv.) were added, and the obtained mixture was milled for 3 hours. The two-step reaction ended with the 56% overall SMR yield (30% SMR yield for the second step). No additional **bPh** was formed in the second step. The monitoring of the first step was the same as in Figure 1. Most of **P1** was formed within the first 2 hours. The last hour of milling in the first step leads to either partial deactivation of the catalyst or its transformation to the less active form. According to the Raman data for the second step, formation of the SMR product **P1** was observed within the first hour and then the reaction almost stops indicating that the active catalyst from the first step was mostly inactivated.

Hence, in the examined solid-state SMR, the formation of the active catalyst for the homocoupling is rapid and gives **bPh**. Its transformation to the active catalyst for the cross coupling occurs in parallel. Once formed, the SMR catalyst does not revert to the homocoupling catalytic species but upon reaching the end point of the SMR gradually loses its activity.

## Catalyst

Palladium complexes (Scheme 3) containing *O*-anions (**C1–C3**), halides (**C4–C6**), neutral *N*-ligands (**C7–C13**), and phosphines (**C14–C17**) have been tested as catalysts under standard conditions.

**Catalysts with *O*-anions.**  $[Pd_3(NO_2)(OAc)_3]$  (**C2**) gave 80% yield for the studied reaction similar to **C1** (Scheme 3). *In situ* Raman data shows that the initiation period is shorter, and the product formation is faster for **C2** than for **C1** (Figure 2a). At least one bond needs to be broken for **C1** and **C2** to enter the reaction. Even though both are trinuclear, opening of the **C2** structure is more accessible due to its asymmetric structure than for the symmetric trimer **C1**.<sup>[54,55]</sup> Namely, due to the *trans* effect of the coordinated nitrite, some bonds around the Pd center that binds nitrite are more or less susceptible to breaking, which is necessary for bonding other compounds.<sup>[54,55]</sup>

Monomeric *O,O*-chelate, palladium(II) acetylacetonate ( $Pd(acac)_2$ , **C3**) gives a moderate yield (51%). The corresponding Raman profile (Figure 2d) shows a long induction time and slow product formation. This result is attributed to the stability of the chelate rings that disfavors the reaction of **C3** with ligands in the reaction mixture (e.g. substrate and PBA) that need to be

coordinated to achieve the coupling. Consequently, the catalytic activity of **C3** is lower.

**“Ligandless” halide catalysts.** Monomeric (**C4**,  $K_2PdCl_4$ ), hexameric (**C5**,  $\beta$ - $PdCl_2$ ) and polymeric (**C6**,  $PdBr_2$ ) halides have been tested under standard conditions. Complexes **C4–C6**, regardless of their structure, give almost the same yield in the 88–90% (Scheme 3). However, formation of the product **P1** is slower than with **C1** and depends on the halide structure. According to the Raman reaction profiles (Figure 2b), the evolution of **P1** is faster in the order: **C6** (polymer) < **C5** (hexamer) < **C4** (monomer). The obtained order agrees with the availability of the metal center to bond ligands. More facile bonding of the ligand to the palladium is expected in the monomeric than in the polymeric structure. Thus, more metal centers are initially available for the reaction using the monomeric rather than the polymeric catalyst. This tends to be equalized as the reaction progresses by breaking the polymer.

The collected data confirmed that both neutral and anionic halide palladium species are viable catalysts for the studied reaction. Thus, the coupling would likely continue if anions in the catalyst were exchanged during milling<sup>[43]</sup> by the released bromides originating from the substrate.<sup>[26]</sup>

Considering that the bromide formed in the coupling reaction may exchange with the ligands bound to the palladium, we have added KBr (0.50 equiv. with respect to **1**) to the reaction catalyzed by **C1** to further test the effect of bromides. The SMR yield was 91% and, according to the *in situ* Raman data, initiation was much shorter (< 5 minutes) and was followed by faster conversion of **1** to **P1**. This result could be attributed to the easier breaking of the trimeric structure of the catalyst **C1** in the presence of the bromide from the start of the reaction.

***N*-ligand catalyst.** Complex  $[Pd(MeCN)_4](BF_4)_2$  (**C7**) gives a high 94% yield (Scheme 3, Figure 2b). Due to its ionic structure with four easily-exchangeable MeCN ligands, the metal center readily coordinates available ligands from the reaction mixture. Thus, **C7** is most likely transformed into the bromide complex due to the bromide accumulation during the reaction.<sup>[40–43]</sup>

**Mixed-ligand catalysts.** Diverse complexes containing halides and/or *O*- and *N*-ligands (**C8–C13**, Scheme 3) have been tested.

The reaction with *trans*- $Pd(OTs)_2(MeCN)_2$  (**C8**) is fast (Figure 2a) and affords **P1** in a 94% yield (Scheme 3). The excellent activity of **C8** could be attributed to the presence of the tosylate ligands which most likely affect the transmetalation step or bromide elimination after the oxidative addition of **1** to the catalyst.

A mixed halide/*N*-ligand complex *trans*- $PdCl_2(MeCN)_2$  (**C9**) gives a comparable yield to the examined halides **C4–C6** (Scheme 3). Time-resolved product formation is similar to that observed for **C1** (Figure 2). The complex **C9** contains two loosely coordinated MeCN released to the mixture during reaction. The volume of MeCN (ca. 2  $\mu$ L) released from the catalyst is too low to cause a change in the product formation due to presence of a liquid (*i.e.* LAG effect).<sup>[17–19]</sup>

*Trans*- $PdCl_2(DMAP)_2$  (**C10**) containing a coordinated strong organic base, 4-(*N,N*-dimethylamino)pyridine (DMAP), is the

most effective among all tested catalysts for the studied reaction, giving a 96% yield (Scheme 3). According to the Raman monitoring of the reaction catalyzed by **C10**, an induction period of about 40 minutes is followed by the rapid conversion of the substrate in the next hour (Figure 2c).

The induction period for *trans*-PdCl<sub>2</sub>(Azb)<sub>2</sub> (**C11**) is similar to that for **C10** but the conversion to **P1** is slower (Figure 2c). The reaction ends with an 83% yield (Scheme 3) showing that azobenzene complexes that may form *in situ* in presence of other catalysts are also viable (pre)catalysts.

Apart from the monodentate *N*-ligands, we have tested *N,N*-chelate complexes **C12** and **C13** containing benzene-1,2-diamine and 2,2'-bipyridine (bpy), respectively (Scheme 3). Coupling catalyzed by the primary amine complex **C12** has an induction period of about 40 minutes upon which the 82% yield is achieved in 3 hours (Figure 2d). On the other hand, the reaction using **C13** shows a long induction of over an hour after which a steady but slow formation of **P1** follows, similar to that observed for the *O,O*-chelate complex **C3** (Figure 2d). The reaction with **C13** achieves only 35% yield.

These results indicate that the catalytic activity of the *N,N*-chelate complexes in the solid-state SMR varies substantially and depends on the *N*-ligand structure and properties where the stability of the chelate ring may play a crucial role. Moreover, the chelate complexes **C3** and **C12** (similar to the highly-active **C7**) gave less **bPh** relative to the **P1** (molar ratio **P1/bPh** is ca. 90/10) than complexes with monodentate ligands (Table S2).

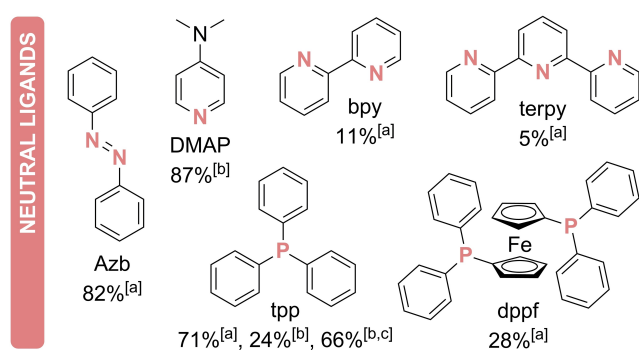
To test if *N,N*-chelating ligands would act similarly if used as additives under standard conditions using **C1**, we have tested bpy and terpyridine (terpy). Almost complete deactivation of the catalyst is observed for the reaction with 0.05 equiv. of bpy (yield 11%) or terpyridine (terpy, yield 5%, Scheme 4). Poor conversion to **P1** (and **bPh**) shows that these *N*-ligands react rapidly and selectively with **C1** and form stable species with poor catalytic activity for the studied coupling in the solid state. Moreover, using the examined *N,N*-chelating ligands as additives to **C1** proved worse than using the *N,N*-chelate halide complex as the catalyst (see Schemes 3 and 4).

**Phosphine catalysts.** The least active catalysts under the applied conditions are common phosphine palladium com-

plexes **C14–C16**. Regardless of the oxidation state of the metal, *i.e.*, Pd(0) or Pd(II), these complexes lead to poor conversion of **1** to **P1**, with yields of 28–30% after 3 hours of milling (Scheme 3). Silica-based catalyst **C17**<sup>[52]</sup> gave a 30% yield (average of two runs) with the time-resolved product formation comparable to other tested phosphine catalysts **C14–C16** (Figure 2d).

To further examine the influence of phosphines, we have tested monodentate *P*-ligand triphenylphosphine (tpp, PPh<sub>3</sub>) and bidentate 1,1'-bis(diphenylphosphino)ferrocene (dppf) as additives in the reaction catalyzed by **C1**. Adding these phosphines in a stoichiometric amount with regard to **C14** or **C15** resulted in a reduced yield (Scheme 4), which is close to the yields obtained using the isolated **C14** or **C15** (Scheme 3). Even one equivalent of tpp with respect to palladium (*i.e.* 0.050 equiv. to **1**) lowers the yield of **P1** to 71%, while two equivalents of tpp (*i.e.* 0.10 equiv. to **1**) give 24% of **P1**. The amount of **bPh** is similar as in the reactions without additives, although a considerable amount of the unreacted PBA is present in the reaction mixture. Therefore, the phosphine additives rapidly reduce the catalytic activity of palladium. These results are consistent with several published reports on mechanochemically-induced SMR under NG conditions without additives<sup>[20,23]</sup> and indicate that the palladium phosphine complexes may give poor results in the solid state, although they are common catalysts in solution. For example, the solution-based coupling of 4-iodoazobenzene (**3**) with the boronic acid derivative catalyzed by **C16** affords the cross coupling product in a 95% yield after 24 hours at 90 °C under nitrogen atmosphere.<sup>[56]</sup> This indicated that the reaction time might be too short. Indeed, the time-resolved Raman plots for the phosphine catalysts (Figure 2d) show that the reaction continues after 3 hours. To check this, we have repeated the reactions using (i) the catalyst **C14** (0.050 equiv.), and (ii) the catalyst **C1** (0.050 equiv.) and the additive tpp (0.10 equiv.) and milled for 12 hours. The yields for these reactions are twice as high as at 3 hours (61 and 66% for conditions (i) and (ii)). *In situ* Raman data for the reaction with **C14** shows that the reaction is completed within 8 hours. Thus, the catalytic activity of the phosphine complexes in the solid-state SMR is lower than that of other types of catalysts.

*In summary*, the best catalysts for the solid-state SMR contain monodentate *N*-ligands. Readily available halide complexes are also a good choice for the catalyst due to their reactivity and high yields. Catalyst activation is slower in the solid-state reactions if the catalyst contains strongly bound ligands (chelating and/or phosphines). The catalytic activity of chelate complexes depends on the chelating ligand's structure. It should be kept in mind that these catalysts could be useful in the solid state as they might favor SMR over the boronic acid homocoupling, thus reducing the primary side reaction.



**Scheme 4.** NMR yields of SMR under standard conditions with neutral ligands as additives. <sup>[a]</sup> 0.050 equiv. and <sup>[b]</sup> 0.10 equiv. of the ligand with respect to the substrate **1**. <sup>[c]</sup> Reaction time was 12 hours.

## Base

After examining the catalysts, we have tested how different reaction conditions may influence the activity of the common catalyst **C1**.

First, we have examined how a different base can affect the solid-state SMR. Apart from  $K_2CO_3$  used in the standard setup, we have selected common inorganic and organic bases (Scheme 5): an inorganic salt (potassium phosphate monohydrate,  $K_3PO_4 \cdot H_2O$ ), and four amines (pyridine (py), DMAP, 1,4-diazabicyclo[2.2.2]octane (DABCO) and 1,8-bis(*N,N*-dimethylamino)naphthalene (the proton sponge)).

**Inorganic base.** If  $K_3PO_4 \cdot H_2O$  is used instead of  $K_2CO_3$  (Scheme 5), an almost quantitative yield is obtained. However, the reaction is considerably slower (Figure S18). Besides the structure of the anion, this increase can be also attributed to the release of water (17.3  $\mu$ L for 2.4 equiv. of  $K_3PO_4 \cdot H_2O$  with regard to **1**). To investigate this, we have used water as an additive in the coupling reaction under standard conditions (*i.e.*,  $K_2CO_3$  as a base). The yields of the LAG- $H_2O$  reactions with 0.50 and 2.4 equiv. of  $H_2O$  improved to 88% and 98%, in agreement with the previous study of the SMR under LAG conditions.<sup>[23,26-28]</sup> Time-resolved product formation observed by Raman spectroscopy showed that water shortened the initiation period and accelerated the reaction (Figure 3b). Apart from the LAG effect, this could be rationalized by the effect of water facilitating the formation of trihydroxoborate ( $PhB(OH)_3^-$ ) or hydroxo Pd-species that enter the transmetalation.<sup>[5,23,46-51]</sup>

BASES	$K_2CO_3$	py	DMAP	DABCO	proton sponge
	84% <sup>[a]</sup> 98% <sup>[b]</sup>	0% <sup>[a,c]</sup>	0% <sup>[a,c,d]</sup>	0% <sup>[a]</sup>	20% <sup>[a]</sup>
$K_3PO_4 \cdot H_2O$	97% <sup>[a]</sup>	11% <sup>[e]</sup>	4% <sup>[e]</sup>	58% <sup>[c]</sup>	93% <sup>[c]</sup>
MeCN	88% <sup>[e]</sup>	42% <sup>[f]</sup>	87% <sup>[f]</sup>		91% <sup>[e]</sup>

**Scheme 5.** NMR yields of SMR under standard conditions with different bases (data in black) or basic additives (orange). Base: <sup>[a]</sup> 1<sup>st</sup> step: 2.4 equiv. of the base (no  $K_2CO_3$  in the mixture for bases other than  $K_2CO_3$ ), <sup>[b]</sup> 2<sup>nd</sup> step: 2.4 equiv. of water added, <sup>[c]</sup> 2<sup>nd</sup> step: 2.4 equiv. of  $K_2CO_3$  added, <sup>[d]</sup> 3<sup>rd</sup> step: 2.4 equiv. of water added. Basic additives: <sup>[e]</sup> 1<sup>st</sup> step: 0.50 equiv. of the base and 2.4 equiv. of  $K_2CO_3$ , <sup>[f]</sup> 1<sup>st</sup> step: 0.10 equiv. of the base and 2.4 equiv. of  $K_2CO_3$ . Each step was milled for 3 hours with the catalyst **C1**.

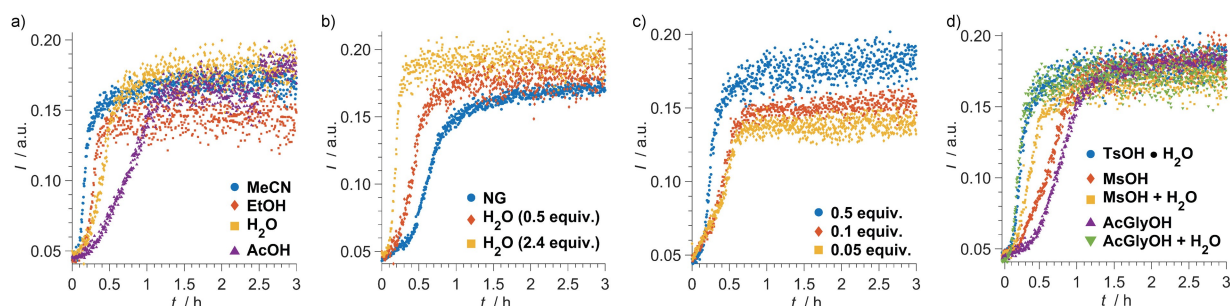


**Figure 3.** Time-resolved Raman intensities at  $1599\text{ cm}^{-1}$  for reactions under standard conditions with added: a) liquid additive (0.5 equiv.), b) water (no water, 0.50 equiv. and 2.4 equiv.), c) TsOH- $H_2O$  (0.50, 0.10 or 0.050 equiv.), and d) acid (0.50 equiv.) or acid (0.50 equiv.) + water (0.50 equiv.).

**Organic base.** The organic base or basic additive may (*i*) alter the activity of the catalyst by changing its structure due to coordination of the base to the palladium and (*ii*) consume PBA by favoring the formation of B–N boroxine adducts with the base which would influence the transmetalation step. Both processes, *i.e.* exchange of ligand(s) on palladium<sup>[43]</sup> as well as the B–N boroxine adducts synthesis *via* the amine-facilitated trimerization of PBA,<sup>[57]</sup> have been recently described. We note that the Raman spectra of the reaction mixtures mainly contain strong bands of the azobenzene compounds which hinders a reliable *in situ* observation of the adduct formation due to their inherently weak Raman bands.<sup>[57]</sup>

Addition of the proton sponge, a sterically hindered strong organic base, lowers the yield to 20% (Scheme 5). This is improved to 93% if  $K_2CO_3$  (2.4 equiv.) is added and milled further for 3 hours. The proton sponge can loosely coordinate to the palladium.<sup>[58]</sup> In addition, according to the Raman monitoring of milling an equimolar mixture of the proton sponge and PBA, a B–N adduct is not formed. However, the hydrogen-bonded assembly of the proton sponge and PBA may form during milling and might not be observed in solution. The mentioned interactions of the proton sponge can influence the solid-state SMR.

The coupling is completely impaired by 2.4 equivalents of py, DMAP or DABCO. No conversion of **1** to the product and no **bPh** has been observed. This could be attributed to the deactivation of the catalyst as palladium readily reacts with *N*-donors giving stable complexes. Almost quantitative SMR using *trans*-PdCl<sub>2</sub>(DMAP)<sub>2</sub> (**C10**, 96%, Scheme 3) shows that coordination of the amine to the metal center cannot account for the observed deteriorating influence of the *N*-donor bases. However, soon after the milling started, <sup>1</sup>H NMR of the reaction mixture with **C1** and DMAP shows signals of the B–N adduct ( $PhBO_3$ )-DMAP.<sup>[57]</sup> These results suggest that the B–N adducts do not act as the PBA source. To examine this, we have used ( $PhBO_3$ )-py instead of PBA in the reaction catalyzed by **C1**. Indeed, no homo- or cross coupling occurred. Thus, rapid *in situ* formation of the B–N adducts with the applied base (py, DMAP or DABCO) stops the reaction as all PBA is consumed.

We have also performed the two-step one-pot couplings where in the first step, we have used only the organic base, py, DMAP or DABCO (2.4 equiv.). No coupling occurred (Scheme 5). Then, we have added  $K_2CO_3$  (2.4 equiv.) to each reaction

mixture and milled for 3 hours more. The yield for the reaction with DABCO/ $K_2CO_3$  is 58% for **P1**. In contrast, no **P1** and no **bPh** are detected after the two-step SMR using py/ $K_2CO_3$  and DMAP/ $K_2CO_3$  even after milling with water as an additive. These results indicate that adding  $K_2CO_3$  to the mixture containing DABCO at least partially leads to the breaking of the B—N adduct whereas for the py and DMAP no reaction occurs. This can be attributed to the previously described difference in the structure of the B—N adducts with py and DMAP compared to that with DABCO.<sup>[57]</sup> Namely, py derivatives form  $(PhBO)_3 \cdot py$  and  $(PhBO)_3 \cdot DMAP$  whereas with DABCO, the amine-bridged adduct  $(PhBO)_3 \cdot (DABCO) \cdot (PhBO)_3$  is preferred.

### Basic Additives

MeCN, py, DMAP, and the proton sponge have been tested as additives in the solid-state SMR catalyzed by **C1** (Scheme 5).

In the LAG-MeCN reaction (10.4  $\mu$ L of MeCN, 0.50 equiv. to 1) under standard conditions the yield (88%) is close to the yield for the reaction with **C9** (90%). However, Raman monitoring reveals that the LAG-MeCN reaction proceeds rapidly, with a very short induction period (<2 minutes) and a high conversion rate (Figure 3a). The short preparation for the coupling could be explained by the facile breaking of the trimeric structure of **C1** with the *N*-ligand MeCN.

The SMR proceeds to 91% with 0.50 equiv. of the proton sponge (Scheme 5) indicating that this basic additive supports the coupling. No significant yield change is observed if only 0.050 equiv. of the proton sponge is added, but the reaction is faster according to the *in situ* Raman data (Figures S16 and S17).

On the other hand, adding 0.10 or 0.50 equiv. of py impaired the coupling ending with 42% and 11% yields, respectively (Scheme 5). The strong decrease in the yield, observed with 0.50 equiv. of py is added, is attributed to the rapid formation of the B—N adduct  $(PhBO)_3 \cdot py$ ,<sup>[57]</sup> which has consumed most of the available PBA and thus almost stopped the reaction. This is supported by  $^1H$  NMR spectrum of the reaction mixture with 0.50 equiv. of py that shows signals of  $(PhBO)_3 \cdot py$  (Figure S50).<sup>[57]</sup>

When 0.10 equiv. of DMAP is added, the reaction yield improves slightly to 87% (Scheme 5) if compared to the SMR without additives. This reaction is slower than the reaction without additives but significantly faster than the reaction with **C10** without additives (Figure S16). This indicates that adding a strong external base is beneficial for the yield of the faster reaction and is attributed to the preferential bonding of DMAP to the palladium centers and the formation of a catalytically-active DMAP complex similar to that formed from **C10**. In contrast, adding 0.50 equiv. of DMAP to the mixture blocks the reaction (yield 4%). This amount of DMAP is sufficient for the complete reaction with the catalyst and with PBA by forming of  $(PhBO)_3 \cdot DMAP$ .<sup>[57]</sup> The presence of  $(PhBO)_3 \cdot DMAP$  in the reaction mixtures has been confirmed by  $^1H$  NMR (Figure S49).

*In summary*, inorganic bases promote the solid-state cross coupling especially if water is added. Care should be taken

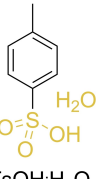
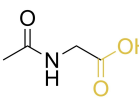
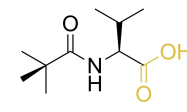
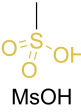
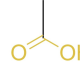
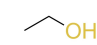
when adding the organic base. The probable interaction of the amines with PBA trapping the PBA in the B—N boroxine adduct should be kept in mind, as it may stop the solid-state SMR.

### Acidic Additives

Water introduced to the reaction mixture acts beneficially to the reaction course which prompted us to expand our list of additives to proton-donor compounds (Scheme 6). Apart from water, we have examined ethanol (EtOH), organic monoprotic acids (acetic acid (AcOH), methanesulphonic acid (MsOH), and toluenesulphonic acid monohydrate (TsOH·H<sub>2</sub>O)), and *N*-monoprotected amino acids (MPAAs,<sup>[59]</sup> *N*-acetylglycine (Ac-Gly-OH) and *N*-(*tert*-butoxycarbonyl)-L-valine (Boc-Val-OH)).

*Water and EtOH* as liquid additives (0.50 equiv.) significantly accelerate the coupling (Figure 3a) and improve the yield to 88% and 86%, respectively (Scheme 6). When the amount of the added water is raised to 2.4 equiv., the induction period is shortened, the conversion is even faster, and the reaction is almost quantitative (Figure 3b). This is consistent with the fact that water accelerates the breaking of the trimeric structure and further reduction of palladium in **C1**, formation of the hydroxo Pd-species and/or easier PBA activation *in situ* by formation of  $PhB(OH)_3$ .<sup>[5,23,29,30,46-51]</sup> The hydroxide anion needed for these reactions originates from the reaction of water with  $K_2CO_3$ . Similarly, EtOH in combination with  $K_2CO_3$  gives ethoxide that is active in transesterification of PBA again increasing the reactivity of PBA for transmetalation.<sup>[23,29,30,46-51]</sup> This result prompted us to check whether this is limited to the model catalyst **C1** or whether adding water would also be advantageous in reactions with other complexes under our experimental conditions. To test this, we have performed the LAG reaction with the poor catalyst **C15** using 2.4 water equivalents. Indeed, the yield improved remarkably to 65% (from 29% for NG). Again, the LAG-H<sub>2</sub>O induction period was shorter, and the evolution of **P1** was faster than that of the NG reaction.

*Carboxylic or sulphonic acids* have a favorable effect and increase the yield to 91–93% (Scheme 6). No clear influence of the aggregate state of the added acid on the yield has been observed. Reactions with TsOH·H<sub>2</sub>O carried out under standard conditions show almost no induction period and are faster

ACIDS	H <sub>2</sub> O			
		88% <sup>[a]</sup> 98% <sup>[e]</sup>	91% <sup>[a]</sup> 88% <sup>[b]</sup> 84% <sup>[c]</sup>	93% <sup>[a]</sup> 88% <sup>[b]</sup> 97% <sup>[d]</sup>
				
	93% <sup>[a]</sup> 92% <sup>[d]</sup>		93% <sup>[a]</sup>	86% <sup>[a]</sup>

**Scheme 6.** NMR yields of SMR under standard conditions with acids as additives. <sup>[a]</sup> 0.50 equiv. of the acid, <sup>[b]</sup> 0.10 equiv. of the acid, <sup>[c]</sup> 0.050 equiv. of the acid, <sup>[d]</sup> 0.50 equiv. of the acid and 0.50 equiv. of H<sub>2</sub>O, and <sup>[e]</sup> 2.4 equiv. of the acid.



(Figure 3c). The less acidic MsOH gives an excellent yield (93%), with the time-resolved product formation of the reaction without additives.

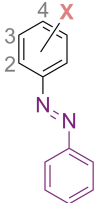
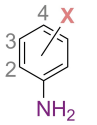
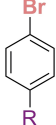
When water is added with MsOH, the reaction accelerates (Figure 3d) and ends with a yield of 92% (Scheme 6). The reaction with added AcOH proceeds slower than without additives (Figure 3a) and ends with 93% (Scheme 6).

MPAAs are known to promote reactions catalyzed by palladium compounds, particularly C1.<sup>[59]</sup> Their action is due to the *O,O*-bidentate coordination to the metal, as the amino group is protected with the acetyl (*e.g.*, Ac-Gly-OH) or the Boc group (*e.g.*, Boc-Val-OH) (Scheme 6), making them ideal for bonding exclusively through the carboxylic end. For both tested MPAAs, Raman monitoring shows a slightly slower reaction than under standard conditions without the additive, similar to the reaction with their parent acid, AcOH (Figure 3).

*In summary*, reactions with acidic additives exhibit slower conversion (except TsOH·H<sub>2</sub>O) but give higher yields than reactions without the additive. The reaction can be accelerated and the yield improved by the addition of water along with the acid. The action of acid additives can be attributed to the more facile activation of the applied catalyst and PBA by transesterification.

## Substrate

Typical organic substrates 1–13 with chloro-, bromo-, and iodosubstituents (Scheme 7) were selected to study the electronic and steric effects for the aromatics undergoing solid-state SMR with PBA. Unfortunately, the Raman spectra collected during the reactions of substrates other than haloazobenzenes (1–5) and 13 showed broad and low-intensity bands that could not be used for a reliable analysis of the reaction course.

SUBSTRATES		1: 4-Br, 44% <sup>[a]</sup> , 84% (81% <sup>[b]</sup> ) (P1)
		2: 4-Cl, <1% (P1)
		3: 4-I, 17% (P1)
		4: 3-Br, 87% (81% <sup>[b]</sup> ) (P2)
		5: 2-Br, 62% (58% <sup>[b]</sup> ) (P3)
		6: 4-Br, 55% (52% <sup>[b]</sup> ) (P4)
		7: 4-Cl, <1% (P4)
		8: 4-I, 7% (P4)
		9: 3-Br, 78% (75% <sup>[b]</sup> ) (P5)
		10: 2-Br, 66% (63% <sup>[b]</sup> ) (P6)
		11: R = CHO, 99% <sup>[a]</sup> (97% <sup>[b]</sup> ) (P7)
		12: R = C(=O)(CH <sub>3</sub> ), 96% <sup>[a]</sup> (93% <sup>[b]</sup> ) (P8)
		13: R = NO <sub>2</sub> , >99% <sup>[a]</sup> (98% <sup>[b]</sup> ) (P9)

**Scheme 7.** Substrates 1–13 and NMR yields of SMR under standard conditions for 1–13 giving products P1–P9. Milling for 3 hours unless stated otherwise. Type (Cl, Br or I) and substitution site (position 2, 3 or 4 on the phenyl ring) of the halogen (X) is marked. <sup>[a]</sup> Milling time was 1 hour. <sup>[b]</sup> Isolated yield.

Moreover, products P2 and P3 exhibit similar Raman spectra to 4 and 5 which hindered the *in situ* monitoring of their synthesis.

Poor conversion was obtained using iodosubstrates, while chlorosubstrates did not react with PBA under the reaction conditions studied. Thus, the activity of the organohalides for cross coupling increases in the order of halosubstituents Cl < I < Br for the azobenzene and the aniline substrates. This is in contrast to the usual behavior in the solution-based reactions, where reactivity increases with Cl < Br < I,<sup>[2–4]</sup> but confirms the literature findings in the solid state under NG conditions.<sup>[20,22]</sup>

In a common description of the SMR mechanism the oxidative addition of the substrate to the catalyst is considered as the rate-determining step.<sup>[2–5]</sup> Reactivity of the halosubstrates is connected with the C–X bond energies (Cl > Br > I) as they are broken during oxidative addition. However, recent findings involving the “ligand-free” SMR of chlorosubstrates suggest that the oxidative addition could be reversible.<sup>[60]</sup> Moreover, a dynamic “cocktail-type” stabilization of metal species that was observed and characterized in solution during SMR of the bromo- and iodosubstrates, but not of the chlorosubstrates, influences the overall reactivity of halosubstrates along with their C–X bond energies.<sup>[61]</sup> Another important effect, especially at temperatures below 50 °C, is the reversibility of the transmetalation and influence of exogenous halides (formed during the reaction) that bind to the Pd center in intermediate species under “ligand-free” conditions, increasingly disfavoring the formation of the hydroxo Pd-species reactive in the transmetalation.<sup>[62–65]</sup> The trend in the equilibrium ratio of hydroxo- and halido Pd-species is opposite to the stability order of the Pd–X complexes.<sup>[62–65]</sup> This could lead to bromosubstrates being the most reactive aryl halides and, thus, the best choice for the solid-state SMR conducted under “ligand-free” conditions. In addition, other effects during the solid-state reaction could lead to differences in the stabilization of the reactive species participating in the catalytic cycle, such as the recently suggested hydrogen bonding of boronic acids and Pd-halide pre-transmetalation species that also depends on the halide type.<sup>[66]</sup>

Next, the yield increases in the order of the *p*-substituents on the halophenyl ring: NH<sub>2</sub> (aniline) < PhN=N (azobenzene) < C(=O)CH<sub>3</sub> (acetophenone) < CHO (benzaldehyde) < NO<sub>2</sub> (benzene). The order follows the increase of the electron-withdrawing effect of the *p*-substituent. The insertion of palladium into the C–Br bond is easy when the bond is weak, *i.e.*, electron-deficient. This was also confirmed by *in situ* monitoring of the reactions (Figure S28). The fastest coupling giving the quantitative yield (> 99%) was achieved for a highly reactive substrate, *i.e.*, 1-bromo-4-nitrobenzene (13). Formation of P9 was followed using a medium-intensity Raman band at 1289 cm<sup>−1</sup> corresponding to a newly formed C–C bond in P9 (Figure 4). In addition, the phenyl C=C stretching band of 13 located at 1569 cm<sup>−1</sup> shifts to 1598 cm<sup>−1</sup> for P9, while the broad band located at about 1345 cm<sup>−1</sup> and corresponding to the symmetric stretch of the nitro group narrows during the reaction. According to the Raman data, the reaction of 13 with

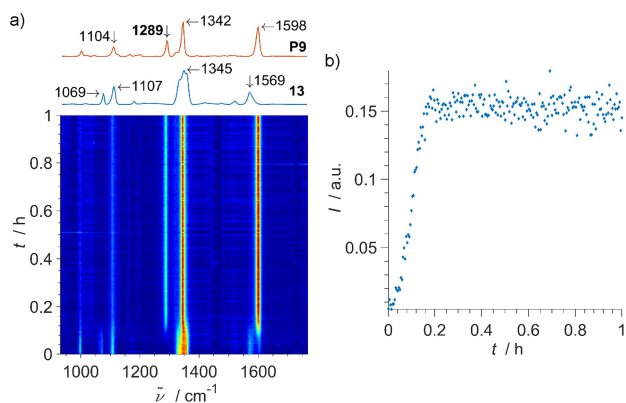


**Figure 4.** a) 2D plot of the time-resolved Raman monitoring of the mechanochemically-induced Suzuki-Miyaura coupling of **13** (0.40 mmol, 1 equiv.) with PBA (1.3 equiv.) catalyzed by **C1** (0.050 equiv.) using  $K_2CO_3$  (2.4 equiv.) as the base and silica (250 mg) as the milling auxiliary ("standard conditions"). Selected part of the Raman spectra of **13** and the product **P9** with a marked characteristic band of **P9**. b) Time-resolved Raman intensities at  $1289\text{ cm}^{-1}$  during the reaction.

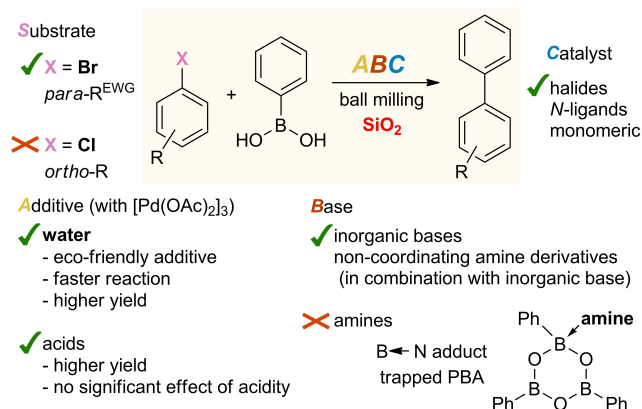
PBA under standard conditions was complete within 20 minutes.

The coupling products of *m*-bromosubstrates **4** and **9** were isolated in 87% and 78%, respectively (Scheme 7). The yields of the sterically demanding *o*-substrates **5** and **10**, were moderate, *i.e.*, 62% and 66%, respectively (Scheme 7). Thus, the coupling efficiency concerning the site of bromosubstitution on the phenyl ring grows in the order *ortho*  $\ll$  *para*  $<$  *meta* to the sterically-demanding group.

*In summary*, structurally different aryl bromides and iodides were successfully employed as substrates for the solid-state Suzuki-Miyaura cross coupling. The best results can be expected for bromosubstrates with electron-deficient substituents.

## Conclusions

Raman monitoring, the key method for following the solid-state chemical transformation *in situ*, was used for the first time to monitor the Suzuki-Miyaura reaction. The gathered data has revealed how diverse compounds used as Additives, the Base, the Catalyst, and the substrate affect the studied cross coupling (Scheme 8). Analysis of the ABCs effects shows that the LAG- $H_2O$  reaction of the bromosubstrate, the boronic acid and the inorganic salt as a base using easily-available palladium halides or complexes with *N*-ligands as catalysts and silica as the milling auxiliary should be the first choice of the milling method for a common stable substrate. Longer activation and lower activity of the palladium complexes that contain strongly bound ligands, *e.g.*, chelating ligands and phosphines, lead to a slow reaction usually with a poor yield. Amines without the added inorganic salt strongly impair the coupling. However, if an organic base is needed along with the inorganic base, addition of a non-coordinating amine (like the proton sponge), that would also not interact with the boronic acid, is preferred.



**Scheme 8.** Guidelines for the mechanochemically-induced Suzuki-Miyaura reaction under reaction conditions similar to those examined in this work. EWG is the electron-withdrawing group.

Acidic additives result in a slower but more efficient cross coupling.

This presented study should facilitate the future design of the solid-state Suzuki-Miyaura reaction. Using the gained in-depth knowledge, the reaction design should be based on a well-considered selection of the reaction mixture components. This should allow faster and finer tuning of the reaction and lead to a shorter list of required trials to achieve a satisfactory synthetic result. Therefore, the improvement in pre-synthetic logic presented here saves resources and follows the fundamental green principles in chemistry. If any additional steric demands or reactivity issues occur regarding the reaction components, additional screening of the reaction conditions guided by the herein obtained results is advised.

## Acknowledgments

Financial support and PhD position for M. P. were provided by the Croatian Science Foundation (grants IP-2019-04-9951 and DOK-2020-01-7515). We thank Dr Sunčica Roca and Ms Nikolina Višić for the NMR measurements. Assist. Prof. Nikola Cindro is gratefully acknowledged for providing the silica-based catalyst. We thank Dr Ivan Halasz for help with the PXRD measurements and valuable discussions.

## Conflict of Interests

The authors declare no conflict of interest.

## Data Availability Statement

The data that support the findings of this study are available from the corresponding author upon reasonable request.

**Keywords:** Additives · *In situ* monitoring · Mechanochemistry · Raman spectroscopy · Suzuki-Miyaura reaction

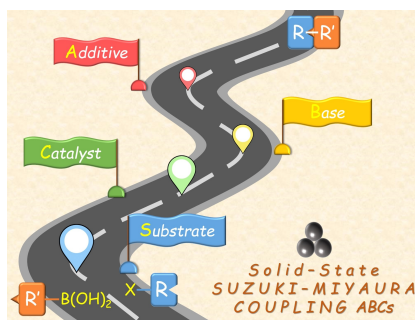
- [1] N. Miyaura, K. Yamada, A. Suzuki, *Tetrahedron Lett.* **1979**, *20*, 3437–3440.
- [2] B. S. Kadu, *Catal. Sci. Technol.* **2021**, *11*, 1186–1221.
- [3] I. P. Beletskaya, F. Alonso, V. Tyurin, *Coord. Chem. Rev.* **2019**, *385*, 137–173.
- [4] A. Biffis, P. Centomo, A. Del Zotto, M. Zecca, *Chem. Rev.* **2018**, *118*, 2249–2295.
- [5] N. T. S. Phan, M. Van Der Sluys, C. W. Jones, *Adv. Synth. Catal.* **2006**, *348*, 609–679.
- [6] S. E. Hooshmand, B. Heidari, R. Sedghi, R. S. Varma, *Green Chem.* **2019**, *21*, 381–405.
- [7] C. Valente, S. Çalimsiz, K. H. Hoi, D. Mallik, M. Sayah, M. G. Organ, *Angew. Chem. Int. Ed.* **2012**, *51*, 3314–3332.
- [8] G. C. Fortman, S. P. Nolan, *Chem. Soc. Rev.* **2011**, *40*, 5151–5169.
- [9] D. A. Alonso, C. Nájera, *Chem. Soc. Rev.* **2010**, *39*, 2891–2902.
- [10] M. Beller, H. Fischer, W. A. Herrmann, K. Öfele, C. Brossmer, *Angew. Chem. Int. Ed.* **1995**, *34*, 1848–1849.
- [11] M. Ashraf, M. S. Ahmad, Y. Inomata, N. Ullah, M. N. Tahir, T. Kida, *Coord. Chem. Rev.* **2023**, *476*, 214928.
- [12] J. Qiu, L. Wang, M. Liu, Q. Shen, J. Tang, *Tetrahedron Lett.* **2011**, *52*, 6489–6491.
- [13] C. Deraedt, D. Astruc, *Acc. Chem. Res.* **2014**, *47*, 494–503.
- [14] F. Scalambra, P. Lorenzo-Luis, I. de los Rios, A. Romerosa, *Coord. Chem. Rev.* **2021**, *443*, 213997.
- [15] K. J. Ardila-Fierro, J. G. Hernández, *ChemSusChem* **2021**, *14*, 2145–2162.
- [16] R. A. Sheldon, *ACS Sustainable Chem. Eng.* **2018**, *6*, 32–48.
- [17] S. L. James, C. J. Adams, C. Bolm, D. Braga, P. Collier, T. Friščić, F. Grepioni, K. D. M. Harris, G. Hyett, W. Jones, A. Krebs, J. Mack, L. Maini, A. G. Orpen, I. P. Parkin, W. C. Shearouse, J. W. Steed, D. C. Waddell, *Chem. Soc. Rev.* **2012**, *41*, 413–447.
- [18] G.-W. Wang, *Chem. Soc. Rev.* **2013**, *42*, 7668–7700.
- [19] N. R. Rightmire, T. P. Hanusa, *Dalton Trans.* **2016**, *45*, 2352–2362.
- [20] S. F. Nielsen, D. Peters, O. Axelsson, *Synth. Commun.* **2000**, *30*, 3501–3509.
- [21] L. M. Klingensmith, N. E. Leadbeater, *Tetrahedron Lett.* **2003**, *44*, 765–768.
- [22] F. Schneider, B. Ondruschka, *ChemSusChem* **2008**, *1*, 622–625.
- [23] Z.-J. Jiang, Z.-H. Li, J.-B. Yu, W.-K. Su, *J. Org. Chem.* **2016**, *81*, 10049–10055.
- [24] X. Yang, C. Wu, W. Su, J. Yu, *Eur. J. Org. Chem.* **2022**, *2022*, e202101440.
- [25] K. Kubota, H. Ito, *Trends Chem.* **2020**, *2*, 1066–1081.
- [26] T. Seo, K. Kubota, H. Ito, *J. Am. Chem. Soc.* **2023**, *145*, 6823–6837.
- [27] T. Seo, N. Toyoshima, K. Kubota, H. Ito, *J. Am. Chem. Soc.* **2021**, *143*, 6165–6175.
- [28] T. Seo, T. Ishiyama, K. Kubota, H. Ito, *Chem. Sci.* **2019**, *10*, 8202–8210.
- [29] W. Pickhardt, C. Beaković, M. Mayer, M. Wohlgemuth, F. J. L. Kraus, M. Etter, S. Grätz, L. Borchardt, *Angew. Chem. Int. Ed.* **2022**, *61*, e202205003.
- [30] K. Yoo, S. Fabig, S. Grätz, L. Borchardt, *Faraday Discuss.* **2023**, *241*, 206–216.
- [31] M. Wohlgemuth, S. Schmidt, M. Mayer, W. Pickhardt, S. Grätz, L. Borchardt, *Chem. Eur. J.* **2023**, *29*, e202301714.
- [32] V. Chantrain, T. Rensch, W. Pickhardt, S. Grätz, L. Borchardt, *Chem. Eur. J.* **2024**, *30*, e202304060.
- [33] O. Trentin, D. Polidoro, A. Perosa, E. Rodríguez-Castellon, D. Rodríguez-Padrón, M. Selva, *Chem.* **2023**, *5*, 1760–1769.
- [34] R. R. A. Bolt, S. E. Raby-Buck, K. Ingram, J. A. Leitch, D. L. Browne, *Angew. Chem. Int. Ed.* **2022**, *61*, e202210508.
- [35] X. Li, Y. Liu, L. Zhang, Y. Dong, Q. Liu, D. Zhang, L. Chen, Z. Zhao, H. Liu, *Green Chem.* **2022**, *24*, 6026–6035.
- [36] S. Lukin, L. S. Germann, T. Friščić, I. Halasz, *Acc. Chem. Res.* **2022**, *55*, 1262–1277.
- [37] S. Lukin, K. Užarević, I. Halasz, *Nat. Protoc.* **2021**, *16*, 3492–3521.
- [38] M. Juribašić, A. Budimir, S. Kazazić, M. Čurić, *Inorg. Chem.* **2013**, *52*, 12749–12757.
- [39] A. Bjelopetrović, D. Barišić, Z. Duvnjak, I. Džajić, M. Juribašić Kulcsár, I. Halasz, M. Martínez, A. Budimir, D. Babić, M. Čurić, *Inorg. Chem.* **2020**, *59*, 17123–17133.
- [40] M. Juribašić, K. Užarević, D. Gracin, M. Čurić, *Chem. Commun.* **2014**, *50*, 10287–10290.
- [41] A. Bjelopetrović, S. Lukin, I. Halasz, K. Užarević, I. Đilović, D. Barišić, A. Budimir, M. Juribašić Kulcsár, M. Čurić, *Chem. Eur. J.* **2018**, *24*, 10672–10682.
- [42] A. Bjelopetrović, D. Barišić, M. Juribašić Kulcsár, I. Halasz, M. Čurić, S. Lukin, *Inorg. Chem. Front.* **2023**, *10*, 6005–6014.
- [43] A. Bjelopetrović, M. Robić, I. Halasz, D. Babić, M. Juribašić Kulcsár, M. Čurić, *Organometallics* **2019**, *38*, 4479–4484.
- [44] M. Walther, W. Kipke, S. Schultze, S. Ghosh, A. Staubitz, *Synthesis* **2021**, *53*, 1213–1228.
- [45] D. Barišić, I. Halasz, A. Bjelopetrović, D. Babić, M. Čurić, *Organometallics* **2022**, *41*, 1284–1294.
- [46] M. C. D'Alterio, È. Casals-Cruañas, N. V. Tzouras, G. Talarico, S. P. Nolan, A. Poater, *Chem. Eur. J.* **2021**, *27*, 13481–13493.
- [47] A. J. J. Lennox, G. C. Lloyd-Jones, *Angew. Chem. Int. Ed.* **2013**, *52*, 7362–7370.
- [48] B. P. Carrow, J. F. Hartwig, *J. Am. Chem. Soc.* **2011**, *133*, 2116–2119.
- [49] C. Amatore, A. Jutand, G. Le Duc, *Chem. Eur. J.* **2011**, *17*, 2492–2503.
- [50] L. A. Adrio, B. N. Nguyen, G. Guilera, A. G. Livingston, K. K. (Mimi) Hii, *Catal. Sci. Technol.* **2012**, *2*, 316–323.
- [51] A. F. Schmidt, A. A. Kurokhtina, E. V. Larina, *Russ. J. Gen. Chem.* **2011**, *81*, 1573–1574.
- [52] M. Lemay, V. Pandarus, M. Simard, O. Marion, L. Tremblay, F. Béland, *Top. Catal.* **2010**, *53*, 1059–1062.
- [53] C. Adamo, C. Amatore, I. Ciofini, A. Jutand, H. Lakmini, *J. Am. Chem. Soc.* **2006**, *128*, 6829–6836.
- [54] J. Váňa, J. Lang, M. Šoltéssová, J. Hanusek, A. Růžička, M. Sedlák, J. Roithová, *Dalton Trans.* **2017**, *46*, 16269–16275.
- [55] V. I. Bakhmutov, J. F. Berry, F. A. Cotton, S. Ibragimov, C. A. Murillo, *Dalton Trans.* **2005**, 1989–1992.
- [56] J. Yang, X. Hu, Z. Jian, *Chin. J. Chem.* **2022**, *40*, 2919–2926.
- [57] M. Pajić, M. Juribašić Kulcsár, *Chem. Eur. J.* **2024**, *30*, e202400190.
- [58] U. Wild, O. Hübner, A. Maronna, M. Enders, E. Kaifer, H. Wadepohl, H. Himmel, *Eur. J. Inorg. Chem.* **2008**, *2008*, 4440–4447.
- [59] Q. Shao, K. Wu, Z. Zhuang, S. Qian, J.-Q. Yu, *Acc. Chem. Res.* **2020**, *53*, 833–851.
- [60] A. F. Schmidt, A. A. Kurokhtina, E. V. Larina, E. V. Vidyayeva, N. A. Lagoda, *J. Organomet. Chem.* **2020**, *929*, 121571.
- [61] A. S. Galushko, D. O. Prima, J. V. Burykina, V. P. Ananikov, *Inorg. Chem. Front.* **2021**, *8*, 620–635.
- [62] J. J. Fuentes-Rivera, M. E. Zick, M. A. Düfert, P. J. Milner, *Org. Process Res. Dev.* **2019**, *23*, 1631–1637.
- [63] C. C. Ho, A. Olding, J. A. Smith, A. C. Bissember, *Organometallics* **2018**, *37*, 1745–1750.
- [64] A. A. Kurokhtina, E. V. Larina, E. V. Yarosh, A. F. Schmidt, *Kinet. Catal.* **2016**, *57*, 373–379.
- [65] C. Amatore, A. Jutand, G. Le Duc, *Chem. Eur. J.* **2011**, *17*, 2492–2503.
- [66] X. Xie, J. Zhang, X.-Q. Song, W. Li, F. Cao, C. Zhou, H. Zhu, L. Li, *Inorg. Chem.* **2024**, *63*, 2606–2615.
- [67] D. Barišić, M. Pajić, I. Halasz, D. Babić, M. Čurić, *Beilstein J. Org. Chem.* **2022**, *18*, 680–687.
- [68] H. Lv, R. D. Laishram, J. Li, Y. Zhou, D. Xu, S. More, Y. Dai, B. Fan, *Green Chem.* **2019**, *21*, 4055–4061.
- [69] D. Formenti, F. Ferretti, F. Ragaini, *ChemCatChem* **2018**, *10*, 148–152.
- [70] G. Kurpiak, A. Walczak, M. Goldyn, J. Harrowfield, A. R. Stefankiewicz, *Inorg. Chem.* **2022**, *61*, 14019–14029.
- [71] P. Liu, X.-J. Feng, R. He, *Tetrahedron* **2010**, *66*, 631–636.
- [72] X. Hu, X. Yang, X. Dai, C. Li, *Adv. Synth. Catal.* **2017**, *359*, 2402–2406.
- [73] J. Do, D. Tan, T. Friščić, *Angew. Chem. Int. Ed.* **2018**, *57*, 2667–2671.
- [74] Y. Wang, R. Xie, L. Huang, Y.-N. Tian, S. Lv, X. Kong, S. Li, *Org. Chem. Front.* **2021**, *8*, 5962–5967.
- [75] K. Shudo, T. Ohta, T. Okamoto, *J. Am. Chem. Soc.* **1981**, *103*, 645–653.
- [76] C. Qian, D. Lin, Y. Deng, X.-Q. Zhang, H. Jiang, G. Miao, X. Tang, W. Zeng, *Org. Biomol. Chem.* **2014**, *12*, 5866–5875.
- [77] S. Mao, Z. Chen, L. Wang, D. B. Khadka, M. Xin, P. Li, S.-Q. Zhang, *J. Org. Chem.* **2019**, *84*, 463–471.
- [78] J. L. Nallasivam, R. A. Fernandes, *Eur. J. Org. Chem.* **2015**, *2015*, 3558–3567.
- [79] K. Užarević, N. Ferdelji, T. Mrla, P. A. Julien, B. Halasz, T. Friščić, I. Halasz, *Chem. Sci.* **2018**, *9*, 2525–2532.

Manuscript received: August 2, 2024

Version of record online: ■■■, ■■■

## RESEARCH ARTICLE

Effects of Additives, Base, Catalyst, and substrate (ABCs) on the mechanochemically-induced Suzuki-Miyaura cross coupling have been studied comparing the time-resolved product formation obtained by *in situ* Raman monitoring of the reactions.



M. Pajić, Dr. D. Barišić, Dr. D. Babić,  
Dr. M. Čurić, Dr. M. Juribašić Kulcsár\*

1 – 12

From *In Situ* Monitoring to Better  
Understanding of the Suzuki-  
Miyaura Cross Coupling in the Solid  
State

